

## Self Autonomous Oscillator: Design, Characterization, Modeling and Computer Analysis Based on NDR Devices

S.A.Kamh<sup>1</sup> and F.A.S.Soliman<sup>2</sup>

<sup>1</sup>Faculty of Women for Arts, Science and Education,  
Ain-Shams University, Heliopolis, Cairo, Egypt.

<sup>2</sup>Nuclear Materials Authority, P.O.Box 2404, El-Horriya 11361,  
Heliopolis, Cairo, Egypt

**ABSTRACT.** Tunnel diode is still regarded as a very useful device in R.F signal processing systems because of its wider band width, temperature stability and lower noise, compared with other diodes. Analytical and experimental investigations and computer program technique has been carried out to control the frequency, amplitude, waveform and output power for different types of tunnel diodes. It is found that the amplitude, frequency and shape of oscillations depend mainly on the biasing condition, and diode-and circuit-parameters. The frequency and amplitude increase with increasing the bias voltage, reaching a maximum value followed by a plateau region, then they decrease at high bias values, which reflects the limits of the dynamic neagative conductance of the tunnel diodes. Results of the sinusoidal oscillations are obtained using InSb tunnel diode having the frequency value of 2.35 MHz. On the other hand, output waveform becomes approximately square wave in case of GaAs samples having the frequency of 0.80 MHz is obtained. The experimental results of the relaxation oscillator show good agreement with the predicted characterization based on the analytical solution and a computer program technique.

Continuous-wave relaxation oscillations have been observed in autonomous self-excited oscillator circuits using InSb and GaAs tunnel diodes, when biased in the negative differential resistance region (Sheng and Sinkkenon 1991). Tunnel diode oscillators are compact r.f generators that have the modest power-supply requirements and can readily tuned by electrical or mechanical means. These diodes hold great promise for high frequency applications because they are not limited by transit-time effects even at microwave frequencies. They typically exhibit 20 to 30 dB lower noise than that achieved with either Gunn-effect or avalanche oscillators and they operate at high dc-to-r.f efficiencies under low dc-bias voltages.

The present study discusses the dependence of tunnel diode relaxation oscillator operation on biasing conditions and circuit -and diode-parameters.

### 1. Analytical Solution:

#### 1.1. Condition of Self-Starting Oscillation:

In the following analysis, the investigated tunnel diode oscillator and its equivalent circuit are shown in Fig. 1 It contains two equal inductive coils ( $L_1$ ,  $L_2$ ), Tunnel diode (T. D) and a load - resistance ( $R_L$ ) and dc-biasing supply. The equivalent circuit parameters are as follows:

-  $Y_0$  : equivalent shunt admittances of the coil “ $Y_1$ ” and the load “ $Y_L$ ” ;  
 $Y_0 = (R_L + j\omega L_c)/(j\omega L_c R_d)$  ..... (1)

-  $Y$  : is the complex shunt admittance of the inductive coils ( $L_1$  and  $L_2$ )

-  $Z_0$  : complex impedance of the tunnel diode circuit =  
 $- R_d / (1 - j\omega C_d R_d)$  ..... (2)

To get the condition of self - starting oscillation, apply Kirchoff's voltage law to the loop circuit of Fig. 1b :

$$I ( Z_0 + 1/Y_0 + 1/Y ) = 0$$

but  $I \neq 0$ , then :

$$Z_0 + 1/Y_0 + 1/Y = 0$$

$$\frac{-R_d (R_d + j\omega L_c) + j\omega L_c R_L (1 - \omega C_d R_d) + j\omega L_c (1 - j\omega C_d R_d) (R_L + j\omega L_c)}{(1 - j\omega C_d R_d) (R_L + j\omega L_c)} = 0$$

$$\frac{(2\omega^2 C_d R_d R_L - (R_d R_L / L_c) - R_L) - \omega^2 L_c + j (2\omega R_L - \omega R_d + \omega^3 L_c C_d R_d)}{((R_L / L_c) + \omega^2 C_d R_d + j (\omega - \omega C_d R_d R_L / L_c))} = 0 \quad \dots (3)$$

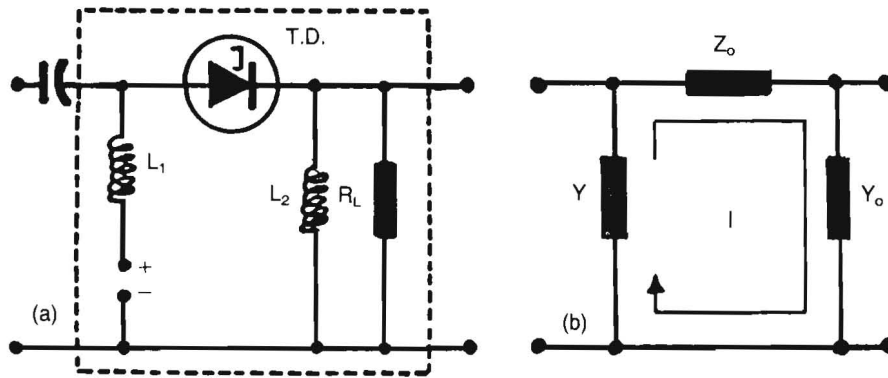


Fig. 1. Circuit Diagram (a) for Tunnel Diode Oscillator and its Equivalent Circuit (b).

Equation 3 can be rewritten in the form:

$$\frac{A_o + JB_o}{C_o + JD_o} = 0 \dots\dots\dots (4)$$

Using the following normalized quantities:

$$W1 = 1/C_d R_d; N = W/W1; S = L_c/C_d R_d^2; W = 2\pi F; \dots\dots\dots (5)$$

$$M = R_L R_d / L_c; Q = 1/C_d \text{ and } X = R_L / L_c$$

Equation 4 becomes ;

$$\frac{(2N^2MS - M - N^2SQ) + J (2NMS - NQ + N^3SQ)}{(X + (N^2QX / M)) + J ((NQX / M) - NX)} = (6)$$

Using the conjugate of the denominator, Equ. 6 becomes ;

$$\left\{ \frac{AC^2 + BD}{C^2 + D^2} + J \left( \frac{BC - AD}{C^2 + D^2} \right) \right\} = 0 \dots\dots\dots (7)$$

Since the whole bracket of Equ. 7 equals zero, then each term must vanish alone, and it is clear from the real and imaginary parts that:

$$AC + BD = 0 \dots\dots\dots (8)$$

and

$$BC - AD = 0 \dots\dots\dots (9)$$

Now, Equ's. 8 and 9 show the conditions of self-starting oscillation that occur in the tunnel diode oscillator circuit. Substituting the values of A,B,C and D in Equ. 9, *i.e.*, the imaginary part of the equation, yields four imaginary roots, which represent unstable oscillator mode, but this is not the case. So, substituting these values in Equ. 8, *i.e.*, the real part gives the following ;

$$N^4 + (1 - (Q/MS)) N^2 - (M/QS) = 0 \dots\dots\dots (10)$$

So, Equ.10 gives the condition of self-starting oscillation and its roots are given as follows;

$$N_{1,4} = \pm \sqrt{(Q/2MS) - (1/2) \pm \sqrt{((1/2) - (Q/2MS))^2 + (M/QS)}} \dots\dots\dots (11)$$

### 1.2. Analytical Results:

It is noticed that, the root N1 has real positive values, and the root N2 has real negative values, while the other two roots are imaginary. So, the oscillator system has one real root, which represents a stable oscillator mode (Kidner *et al.* 1990), and two imaginary roots which represent unstable oscillator mode. The fourth root has negative values which indicates decaying oscillator mode.

#### 1.2.1. The Solution Dependence of Relaxation Oscillations:

Oscillations whose period and shape depend strongly on the energy storage elements of the tank circuit and characteristics of nonlinear element are called "relaxation oscillations". The solution of these systems depends on both; the diode parameters and circuit terms as follows:

##### a) Diode Parameters:

The effects of the diode junction capacitance ( $C_d$ ) and its effective negative resistance ( $R_d$ ) on solution is shown in Fig. 2. Fig. 2 (a) shows that a quasi-linear dependence appears between normalized frequency ( $N=W/W1$ ) and " $R_d$ " values. On the other hand, Fig. 2 (b) shows the dependence of the normalized

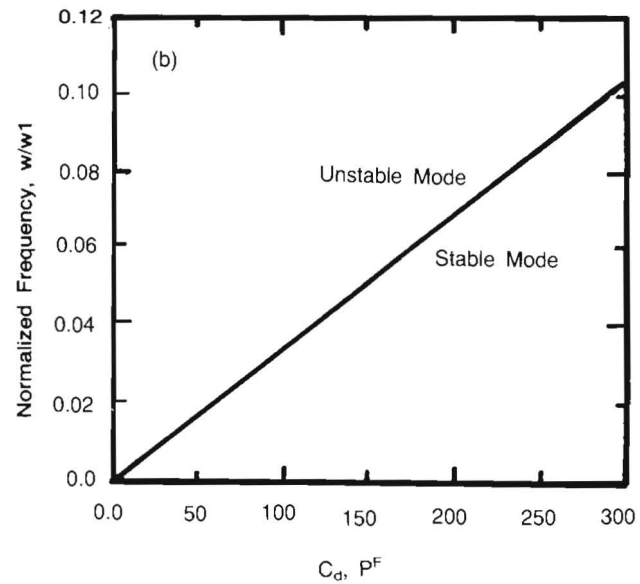
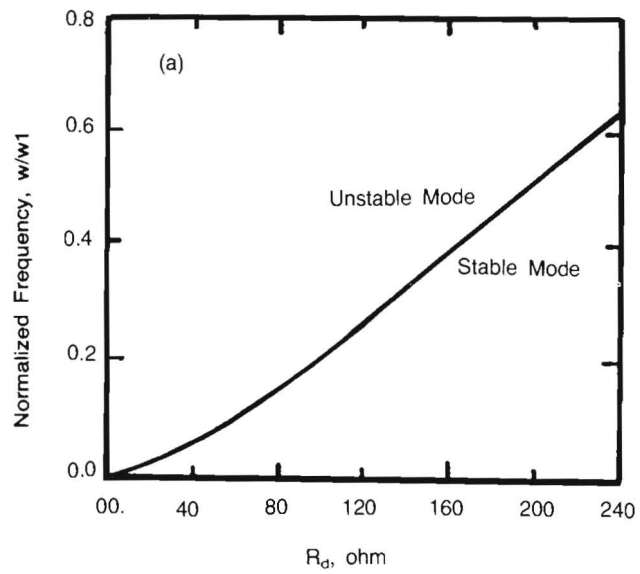


**Fig. 2.** Stability Diagrams of the Oscillator System for Different Diode Parameters. (GaAs; Type A  $\text{N} 301\Gamma$ ).

frequency on  $C_d$  values. It is clear that the frequency of oscillation has a linear dependence on the diode capacitance which shows the importance of using diodes with large  $C_d$  values in constructing the relaxation oscillator systems.

The linear and quasi-linear dependencies of normalized frequency on both " $C_d$ " and " $R_d$ " can be explained applying the well known relations stated in Equ. 5, where:

$$N = 2. \pi. F_{op}. R_d. C_d \dots\dots\dots (12)$$

Where:

$F_{op}$  : operating frequency

The observed quasi-linear deviation is mainly due to the non linearity of the (I-V) curves of the diode and the change in its effective negative conductance (Chow 1946), where:

$$G_{eff} = (9/8). [(I_p - I_v)] / [(V_v - V_p)] \dots\dots\dots (13)$$

Where:

$I_p, V_p$ : peak current and voltage respectively

$I_v, V_v$ : valley current and voltage respectively

On the other hand, linearity shown in Fig. 2 (b) is due to the fact that  $C_d$  value changes linearly with the band of applied bias voltage values within the negative conductance region as given by (Brown 1988, Steazer and Nelson 1961):

$$C_d(V) = K (\varphi - V)^{-1/2} \dots\dots\dots (14)$$

Where:

$K$  : relative dielectric constant;  $1.4 \times 10^{-12}$  volt<sup>1/2</sup>. farad.

$\varphi$  : barrier height

$V$  : bias voltage

b) - Circuit Parameters:

The effects of the circuit parameters (inductance and operating frequency) are calculated and presented in Fig's. 3a and 3b. The first figure shows the dependence of the normalized frequency on the circuit inductance values. The frequency of oscillation is practically inversely proportional to the total circuit inductance " $L_c$ " values, which is true for designing relaxation oscillators, where the oscillation frequency can be expressed in the form (Chow 1964).

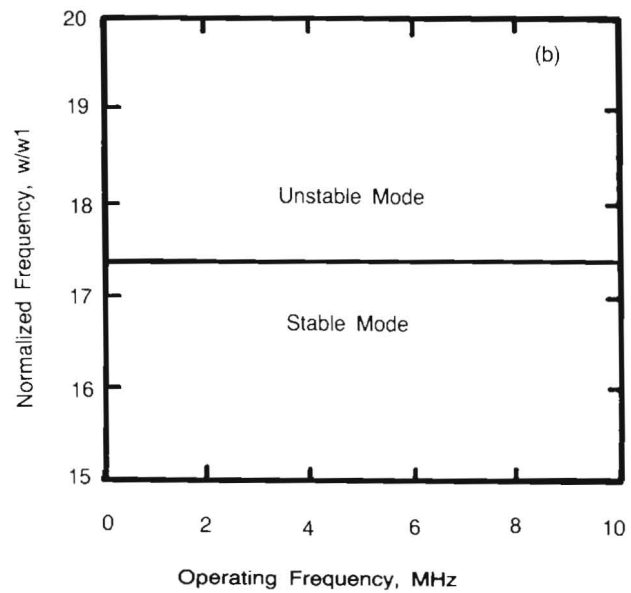
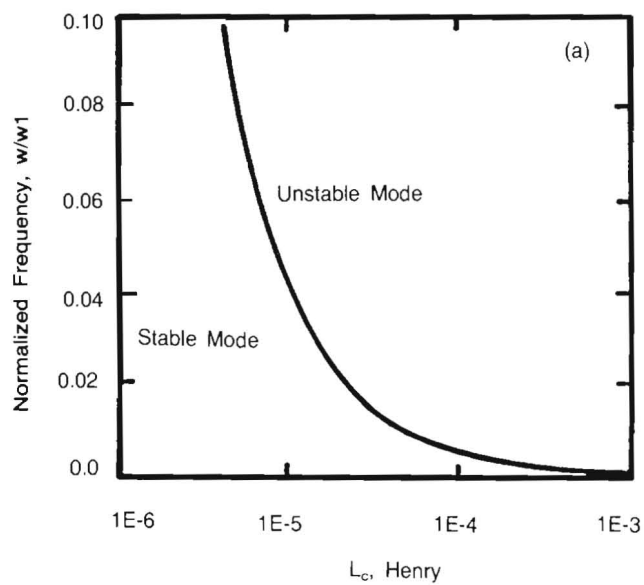


**Fig. 3.** Stability Diagrams of the Oscillator System for Different Circuit Parameters Using GaAs Tunnel Diode.

$$T = (L/R_T) \cdot \ln [(U_o - I_v R_T)/(U_o - I_p R_T)] \dots\dots\dots (15)$$

Where:

$$R_T = R_L + (V_p/I_p) \dots\dots\dots (16)$$

Finally, Fig. 3b shows that the dependence of the normalized frequency on the operating frequency ( $F_{op}$ ) is almost constant.

## 2. Experimental Investigation

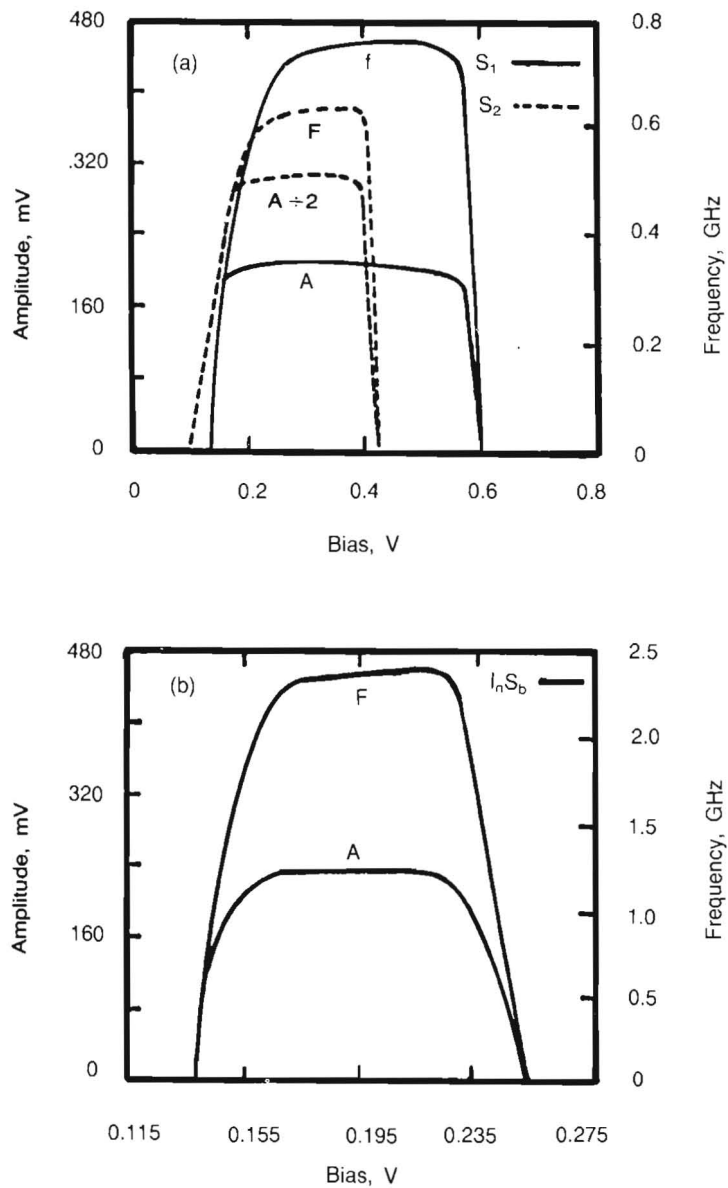
The dependence of both the amplitude (A) and frequency (F) of oscillations on the bias voltage ( $U_o$ ) was investigated, using the circuit shown in Fig. 1a, for diodes with different doping levels and materials (GaAs and InSb).

Comparison study for the behaviour of three different diodes is shown in Fig. 4. It is clear from the figure that for all the investigated samples, the self oscillation starts almost at bias voltage values around 0.145 ( $\pm 5\%$ ) volt. The amplitude (A) of oscillation increases rapidly from zero up to a certain value which depends on the diode type, followed by a plateau region, which was kept up to cutoff point where the oscillation ceasing. Similarly, the frequency (F) follows the same trend as the amplitude, although it exhibits a nearly narrower plateau. The cut off points of the oscillation are shown to be function of the diode type and materials. For the InSb diodes, a cut off bias voltage is around 0.240 volt. On the other hand, for the case of the GaAs samples, this value is observed to be 0.42 and 0.60 volt for the two samples (A  $\nabla$  301r and A  $\nabla$  301  $\Gamma$ ) respectively.

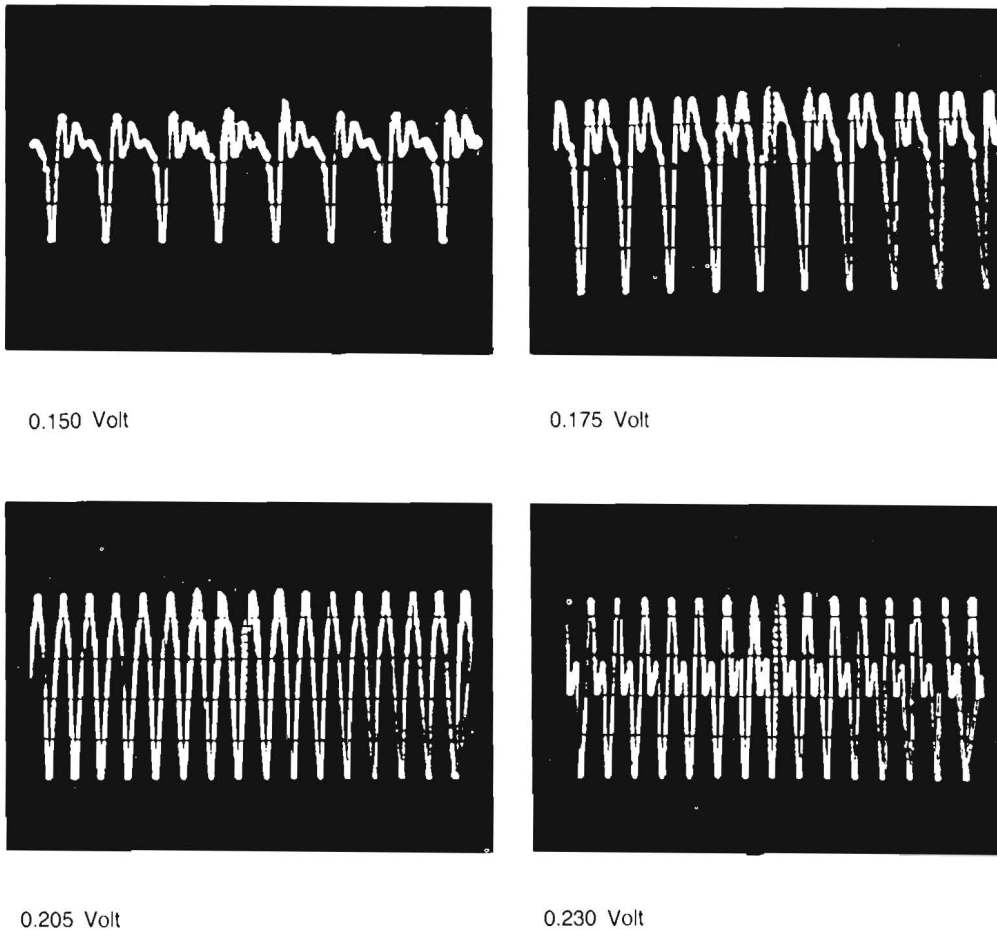
The dependence of the relaxation oscillation waveforms on the bias voltage, for the two diode types (GaAs and InSb), are investigated. Fig. 5 shows oscilloscope tracings of the output of InSb diodes oscillator, under different bias voltage values of 0.150, 0.175, 0.205, and 0.230 volt, respectively. Also, Table 1 summarizes the oscillation characteristics of the investigated samples.

Table 1. Oscillation Characteristics of InSb Tunnel Diode Oscillator

Bias, Volt	$V_p$ , Volt	$V_v$ , Volt	Ampl., Volt	Freq., MHz
0.150	0.14 $\pm$ 5%	0.25 $\pm$ 5%	0.155	1.185
0.175			0.240	1.422
0.205			0.230	2.350
0.230			0.225	2.290



**Fig. 4.** Experimental Dependence of the Amplitude (A) and Frequency (F) on the Bias Voltage for Tunnel Diode with Different (a) Type and (b) Diode Material.



**Fig. 5.** Oscilloscope Tracings of the Output of InSb Tunnel Diode Oscillator Biased at Different Voltage Values.

The oscillations are nearly sinusoidal if the diode is biased around the middle of the negative resistance region. These effects are mainly due to (Brown 1988, Boudrean and Liu 1990).

1. The harmonic content of the output of the oscillator generally changes, because the oscillator swings over different portions of the (I-V) characteristics of the diode at different values of bias. These changes in harmonic content usually lead to changes in the fundamental frequency.

- Changes in bias also cause changes in the effective value of  $C_d$ , because  $C_d$  is voltage dependent (Equ. 14). Variations in frequency resulting from changes in  $C_d$  can be readily estimated by assuming that the effective value of  $C_d$  is the same as its value at the bias point.

When the total circuit inductance of a tunnel diode oscillator is relatively large, the energy stored in this inductance due to the flowing of current can not be dissipated within a short period. The excursion of the diode voltage is forced into the non-linear positive-conductance region of the diode ( I-V ) characteristics. The output waveform becomes approximately square wave, as in case of GaAs samples (Fig. 6).

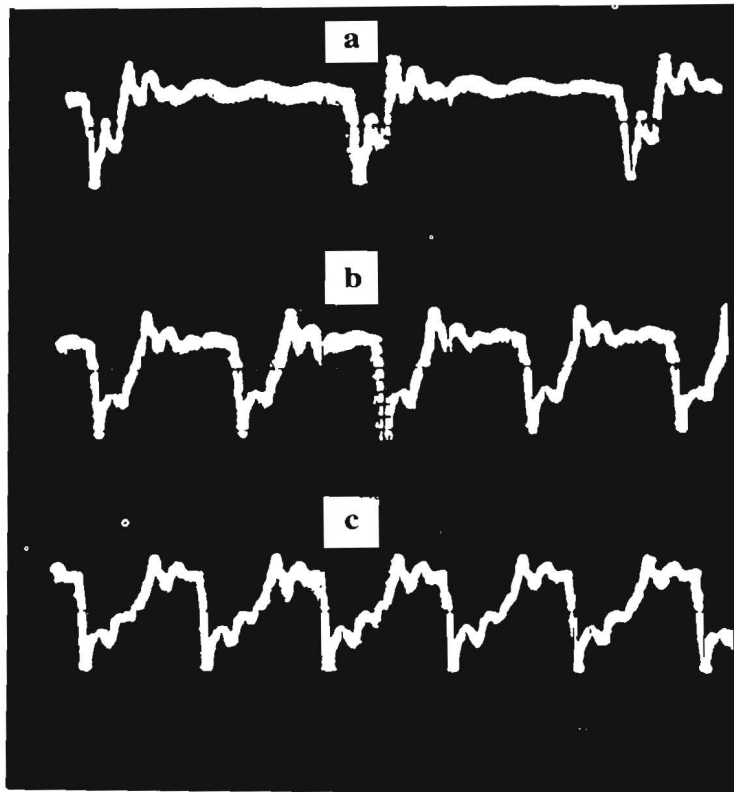


**Fig. 6.** Output Waveforms of GaAs Tunnel Diodes Biased at (a) 0.15 Volt, (b) 0.34 Volt and (c) 0.54 Volt, Respectively.

When the bias point is in the negative - conductance region ( $U = 0.161$  volt) and close to the peak point ( $V_p = 0.150$  volt), the duty ratio of the positive pulse is small, and the repetition rate is also relatively small ( $F = 0.360$  MHz; Fig. 6(a)). For bias values near the middle of the negative conductance region ( $U_o = 0.340$  volt), the duty ratio of the positive pulse is close to 50% and the repetition rate is increased ( $F = 0.620$  MHz; Fig. 6 (b)). Finally, when the bias ( $U_o = 0.541$  volt) is closed to the valley point ( $V_v = 0.70$  volt), the duty ratio is larger than 50% and the repetition rate increases ( $F = 0.80$  MHz ; Fig. 6(c)). On the other hand, and for the investigated bias voltage range, the oscillation amplitude is shown to be approximately constant with a value of  $0.203 (\pm 3\%)$  volt.

GaAs samples characterized with higher electrical parameters ( $V_v$ ,  $I_p/I_v$ ,  $V_{FP}$ ,  $V_v/V_p$ ,  $C_d$  and  $V_{sw}$ ; where  $V_{sw}$  and  $V_{FP}$  are the voltage swing and the forward peak point, respectively) are shown to exhibit the wider bias range than others.

In case of amplitude, which mainly depends on the voltage swing of the devices, it is clearly shown that: If the voltage swing is large, it may go into the positive conductance region. This action produces additional losses and, together with the non-linear characteristics, limits the amplitude of oscillation. It is seen that InSb devices exhibit higher oscillation frequency than that obtained in case of using GaAs ones which is due to the location of the minimum of the conduction band and the maxima of the heavy and light-hole valence bands are all at the center of the "Brillouin zone" (Boudrean and Liu 1990, Van Degrieff and Love 1981). The small forbidden energy gap and effective masses in addition to the high mobility of InSb make it of interest because the high tunneling current density needed for an electronically fast devices can be achieved very readily with low doping concentrations.

Second thought would prompt the realization that the solubilities of the donor and acceptor impurities required to produce the heavily doped regions will be finite and that it might be difficult to obtain an electronically fast tunnel diode with a high energy gap semiconductors (Blaine 1982).

#### **Power Output Consideration:**

We have discussed the various tunnel diodes oscillator circuit, their initial conditions required for oscillation and the frequency, amplitude and waveforms of oscillation. It is also desirable to study the output power of oscillator and the relationship between the output power and the frequency. The tunnel diode can deliver output power up to its cut off frequency as given by (Blaine 1982).

$$P_o = (3/16) [I_p - I_v] [V_v - V_p] [1 - (F_{op}/F_r)] \dots\dots\dots (17)$$

Where:

- $F_r$  : cut off frequency =  $[1/(2 \cdot \pi \cdot |R_m| \cdot C_d)] \cdot [(R_m/R_s)-1]^{1/2}$   
 $R_s$  : spreading resistance  
 $R_m$  : minimum negative resistance

Power output versus frequency of typical tunnel diodes oscillator is shown in Fig. 7 Power values as low as micro watt are obtained from such devices (1020 and 33.8  $\mu$  watt for GaAs and InSb respectively), the matter which is due to that, the active region of tunnel diode is at a much lower voltage than conventional devices (Virk 1987 and Kidnear 1990). This can be clearly observed in case of the investigated GaAs and InSb samples which have comparable active region widths of 0.45 and 0.100 volt, respectively (Fig. 8).

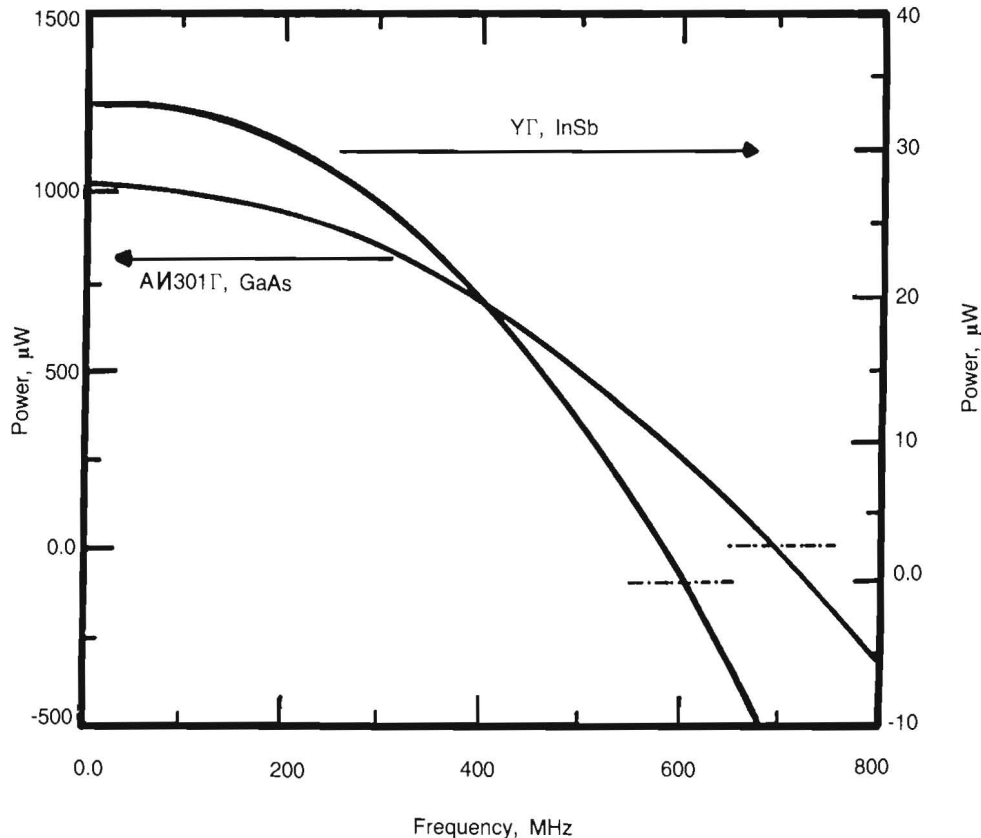


Fig. 7. Output Power Characteristics of Tunnel Diodes.

Actually, Equ. 17 indicates the frequency at which the power absorbed by the positive resistance ( $R_s$ ) is equal to the power that the negative resistance is capable of deriving from the dc battery in the form of an ac signal. This power is frequency dependent because of the shunting effect of  $C_d$  on  $R_d$ . In other words, the ac-current that flows through  $R_s$  at the cut off frequency is much larger than the ac-current flows through  $R_d$ . As a result, it is clear from the curves that at frequencies above cut off level of the device, the real part of the impedance becomes positive, which in turn leads to the fact that the output power is negative.

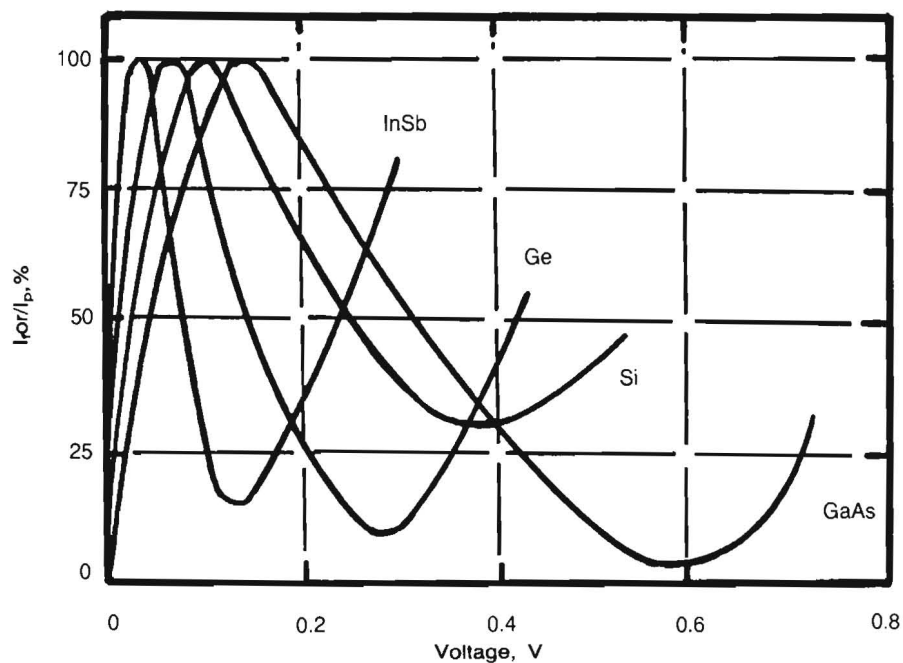


Fig. 8. Current - Voltage Characteristics of Tunnel Diodes Made from Different Semiconductors.

### Conclusions

From the analytical and experimental investigations, the following conclusions could be deduced:

- The amplitude, frequency and shape of oscillations depend mainly on the biasing condition, and diode-and circuit-parameters.

- The frequency and amplitude of the relaxation oscillation increase with increasing the bias voltage, reaching a maximum value followed by a plateau region, then they decrease at higher bias voltage values, which reflects the limits of the dynamic negative resistance of the tunnel diode.
- Sinusoidal oscillations are obtained using tunnel diode of the type  $Y\Gamma$  ; "InSb". Although, actual tunnel diode oscillators like any other physically realizable oscillator, are never purely sinusoidal. On the other hand, output waveform becomes approximately square wave in case of GaAs samples.
- The optimum parameters for the circuit oscillator are:  
 $R_L = 10 \text{ k. ohm}$ ,  $L = 25 \mu\text{H}$ ,  $E_b = 1.5 \text{ volt}$ ,  $R_o = 3 \text{ ohm}$ .

## References

- Blaine, C.** (1982) Tunnel Diode Oscillators, *Microwave Jr. (USA)*, **25** (9): 184-191.
- Boudrean, M.G., and Liu, H.C.** (1990) Effect of the Quantum Inductance on the Equivalent Circuit Model of a Resonant Tunneling Diode, *Super-Lattices and Microstructures (U.K)*, **8**(4): 429-432.
- Brown, E.R.** (1988) High-Speed Resonant-Tunneling Diodes, In: *Proc. of the SPIE. The Intr. Society for optical Eng., (USA)*, **943**: 2-31.
- Chow, F. W.** (1964) *Principles of Tunnel Diode Circuits*; John Wiley and Sons. Inc. 180 p.
- Kidner, C. Mehdi, I. East, J.R., and Haddad, G.I.** (1990) Power and Stability Limitations of Resonant Tunneling Diodes, *IEEE, Trans. MTT*, **38**(7): 864-872.
- Sheng, H.Y and Sinkkenon, J.** (1991) High Frequency Properties of Resonant Tunneling Diodes, *Super-Lattices and Micro-Structures (U.K)*, **9**(4): 537-542.
- Steazer, F. and Nelson, D.E.** (1961) Tunnel-Diode Microwave Oscillators; *Proc. IRE*, **3**: 744-753.
- Van Degrift, C.T. and Love, D.P.** (1981) Modeling of Tunnel Diode Oscillators, *Rev. Sci, Instrum.*, **52**(5): 712-723.
- Virk, R.S.** (1987) Using Tunnel Diode Technology, *MSN Micro. Syst. News Commun. Technol., USA*, **17**(12): 68-75.

(Received 19/04/1993;  
in revised form 07/02/1994)

## التحليل الرياضي لتصميم أنظمة مذبذبات ذاتية التحكم باستخدام ثنائيات الاختراق

سناء عبد التواب قمح<sup>١</sup> و فؤاد عبد المنعم سعد سليمان<sup>٢</sup>

<sup>١</sup> كلية النبات للعلوم والآداب والتربية - جامعة عين شمس - القاهرة  
<sup>٢</sup> هيئة المواد النووية - ص.ب: ٥٣٠ - المعادي ١١٧٢٨ - القاهرة - مصر

أجريت دراسة رياضية وتم وضع نموذج وبرمجة معادلاته على الحاسب الآلي وذلك لتصميم أنظمة مذبذبات ذاتية التحكم باستخدام ثنائيات الاختراق، ساعد البرنامج المقترح على دراسة كافة الجوانب المؤثرة على تشغيل وحدوث التذبذب الذاتي كالتحولات الفيزيائية للنبائط (درجة تركيز الشوائب، نوع مادة الثنائي)، المتغيرات الكهربائية للنبائط، ثوابت الدائرة الكهربائية وظروف تشغيل المذبذب.

بتطبيق النموذج النظري على الدوائر العملية كانت النتائج في تطابق ممتاز مما يعطي انطبعا جيدا على نجاح النموذج الرياضي المقترح طبقاً لبرنامج الحاسب الآلي.